Journal of Statistical Physics, Vol. 32, No. 3, 1983

Simple Models for Bifurcations Creating Horseshoes

J. M. Gambaudo[1] and C. Tresser[2]

Received July 20, 1982

We present a class of simple models for global bifurcations creating horseshoes. Some properties known for Hénon mappings are easily obtained for these models such as, e.g., the existence of nontrivial hyperbolic sets. Kneading sequences techniques allow us to exhibit explicit differences with the global bifurcation diagram for maps of the interval. Explicit examples displaying wild hyperbolic sets and infinitely many sinks are also given as an illustration of the simplicity of these models.

KEY WORDS: Horseshoes; bifurcations; wild hyperbolic sets; infinitely many sinks; Hénon mappings.

1. INTRODUCTION

One of the fundamental problems in bifurcation theory, especially if one is interested to its applications to the onset of turbulence,[17] is to understand the way in which horseshoes[20] are created. Since the introduction and first studies by Hénon[8] of a simple and explicit model for the formation of a horseshoe,[6] there is a controversial belief that strange attractors might appear in the process of formation. However, despite their very simple formula,

$$H_{a,b} : (X, Y) \mapsto (1 - aX^2 + Y, bX) \tag{1}$$

the Hénon mappings are essentially difficult to analyze from the mathematical point of view, and can even be difficult to handle numerically (see, e.g., Refs. 4, 5, and 18).

[1] Laboratoire de Mathématiques, Parc Valrose, 06034 NICE Cedex, France. (L.A. 168, associé au C.N.R.S.)

[2] Laboratoire de Mécanique Statistique, Parc Valrose, 06034 NICE Cedex, France. (L.A. 190, associé au C.N.R.S.)

0022-4715/83/0900-0455$03.00/0

Our goal in this paper is to present a "new" class of simple models for the formation of a horseshoe and to describe their simplest properties. A great advantage of these models is that most nontrivial features known to occur, e.g., for Hénon mappings, can be realized explicitly in this case. One should also mention that models of the same kind have been used before (e.g., Ref. 15), but only in a geometrical way—i.e., no formulas were attached to the construction.

The paper is organized as follows: Section 2 is devoted to the presentation of the models: as well as Hénon mappings, they appear as particular cases of a slight generalization of models proposed by Bowen in Ref. 2.

In Section 3, we take some benefit from the fact that many orbits of our mappings can be understood in terms of a single one-dimensional endomorphism, pertaining to a known one-parameter family. In particular, (Section 3.1), we show how to get, very simply as compared to Hénon's case (see Ref. 21), a horseshoe for the second iterate of the mapping: the hyperbolic structure of the nonwandering set of this horseshoe is straightforward. Note that except when $|b|$ is very small,[9] such results were explicitly proved for Hénon mappings only in the orientation reversing case[7,11,21] and even then, nontrivial hyperbolic sets were merely known to exist (using Ref. 20) and not explicitly described. We also exhibit in Section 3.2 explicit differences in the bifurcation diagram for one-dimensional maps and our mappings.

Finally, in Section 4, we give explicit examples of wild hyperbolic sets [14] (Section 4.1) and of mappings with infinitely many sinks[13] (Section 4.2): the wild hyperbolic sets are constructed using the horseshoes of Section 3.1 and the infinitely many sinks come from orbits described in Section 3.2.

2. PRESENTATION OF THE MODELS

Let

$$f : I \to I$$

be an endomorphism of the unit interval and let

$$\Gamma = \gamma([0,1])$$

be a curve in the unit square $S = I \times I$ with

$$y_2 > y_1 \Rightarrow p_1(\gamma(y_2)) \geqslant p_1(\gamma(y_1))$$

$$p_2(\gamma(y)) = f(y)$$

where p_1 and p_2 are the projections on the x and y axis (e.g., in Ref. 2

Bowen chooses Γ as the graph of f). The mapping

$$\begin{array}{rccc} F_0\colon & S & \longrightarrow & S \\ & (x,y) & \mapsto & \gamma(y) \end{array}$$

is an endomorphism of S whose dynamics is completely described by f. One can extend F_0 to an injective map:

$$F : S \to S$$

by

a. contracting S along its left boundary $\{0\} \times I$ so that $\{0\} \times I$ is no longer necessarily a boundary of the contracted S but so that in any case this contracted strip contains $\{0\} \times I$;

b. arranging the contracted strip along the curve Γ so that $\{0\} \times I$ is precisely mapped onto the curve Γ (see Fig. 1).

The thickening of Γ means that the y-dynamics under Γ is no longer given by a single map of the interval (compare to the case F_0 where the width of the strip is zero everywhere). Applying F successively corresponds to composition of maps "near" f.

The Hénon mappings[8] give concrete examples of this "thickening" construction. We recall[21] that they can be rewritten as

$$(x, y) \mapsto (y, Ry(1 - y) + bx)$$

with (x, y) affine functions of the coordinates (X, Y) used in formula (1), when $(1 + b)^2 + 4a \geqslant 0$ (i.e., when $H_{a,b}$ admits at least a fixed point). More generally, given $f: I \to I$, one gets a "generalized Hénon mapping" by writing

$$\mathcal{F}(x, y) \mapsto (y, f(y) + bx)$$

These mappings have the advantage of being given by very simple formulas. The price one pays is that, because horizontal lines are mapped to vertical ones, one loses almost all control of most of the nonwandering set and the associated invariant manifolds.

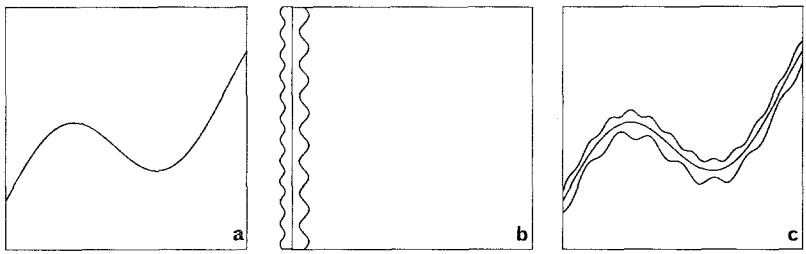

Fig. 1. (a) $\Gamma = \gamma([0, 1])$; (b) S is contracted on a strip along its left side; (c) this strip is mapped along Γ.

The class of models we propose can be defined by requiring that, except for a (narrow) horizontal strip, horizontal lines in the square S be mapped to horizontal lines. Specifically, we consider mappings F of the square S to itself which have the form

$$F(x, y) = (g_y(x), f(y))$$

except for y in a strip $I \times U$. In this formula g_y depends smoothly on y, with $|dg_y/dx| < 1$ and $g_0(0) = 0$; $f: I \to I$ is assumed to be unimodal, taking on its maximum at $c \in]0, 1[$ and one assumes furthermore that $f(0) = f(1) = 0$, so that the origin $0 = (0, 0)$ is a fixed point of F.

Furthermore, $U =]u_m, u_M[$ with $0 < u_m < c < u_M < 1$ and the relation between F and f in $I \times U$ is chosen so that f describes the y transformation of points on all the left boundary of the unit square, i.e.,

$$p_2 F(0, y) = f(y)$$

We shall be mostly concerned with the physically more relevant case when F preserves orientation. Then, in order to make many computations simpler, we shall also impose that the vertical segment $\{0\} \times [0, c]$ be part of the unstable manifold of 0, so that the condition $f(c) = 1$ corresponds to the existence of tangent homoclinic points in the invariant manifolds of 0.

Let us now make some remarks:

1. The y-transformation for a point in $[0, 1] \times U$ will be given by a member of a continuous one-parameter family f_ν, $\nu \in [0, 1]$ with $f_1 \equiv f$: if U is small enough, we obtain that a great part of the y-dynamics of F is described by a single one-dimensional map f;

2. In the limit $U = \{c\}$, F globally preserves the set of horizontal lines with the line $[0, 1] \times \{c\}$ mapped to a single point. Then the y-dynamics of F is completely described by f: F is indeed a skew-product over f given by

$$F(x, y) = (g_y(x), f(y))$$

where g_y is a contraction over horizontal leaves, depending continuously (or as smoothly as one wants) on y, with $\partial g_y/\partial x \to 0$ as $y \to c$. A fairly complete description of this kind of "pinched diffeomorphisms" will be given elsewhere; let us just remark here that in the general case, F appears as a perturbation of such objects (which do have strange attractors with Cantor-like transverse structure when f admits an invariant probabilistic measure absolutely continuous with respect to Lebesgue) instead of a perturbation of a simple one-dimensional map as in the case of generalized Hénon mappings.

Different examples of such mappings will be constructed for different purposes in the sequel of the paper. We have just illustrated in Fig. 2 the main difference between our models and generalized Hénon mappings.

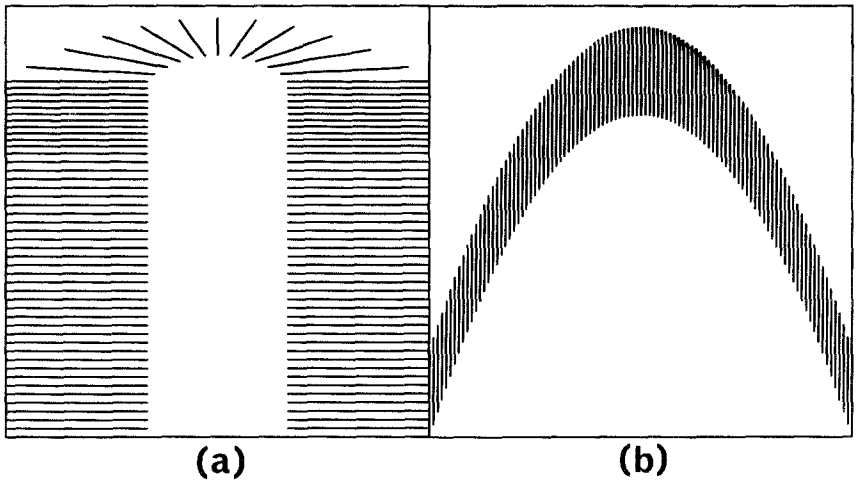

Fig. 2. $F(S)$ for (a) our mappings, (b) Hénon mappings (here $b > 0$). The lines are images of horizontal fibers $[0, 1] \times \{y\}$.

3. SOME SIMPLE CONSEQUENCES OF THE ALMOST PRESERVED HORIZONTAL FOLIATION

In this section, we will be concerned with some orbits in the nonwandering set $\Omega(F)$ which have at most one point in the "bad set" $[0, 1] \times U$. In the first subsection, we will exhibit a hyperbolic set in the complement of $[0, 1] \times U$, for F correctly chosen. In the second subsection, we will consider some periodic orbits with only one point in $[0, 1] \times U$, and give an example of the differences between the bifurcation diagrams for one-dimensional maps and some one-parameter families of diffeomorphisms in the process of formation of a horseshoe.

To make the proofs as simple as possible, we will place unnecessarily strong restrictions on the mappings we consider: in Section 3.1, F will uniformly contract horizontal leaves in the complement of the bad set $[0, 1] \times U$, and in Section 3.2, we will furthermore specify that the maps belong to an explicit five-parameter family.

3.1. A Horseshoe for F^2

Let us write the complement of the bad set

$$S \setminus [0, 1] \times U = C = C_L \cup C_R$$

where C_L (respectively C_R) is the connected part of C below (respectively, above) $[0, 1] \times U$. Then, $F_C = F|_C$ is a map from C to the unit square

given by

$$(x, y) \mapsto (g_y(x), f(y))$$

where g_y is a contraction over horizontal leaves in C. For the sake of simplicity, we shall suppose that

(a)
$$U =]\tfrac{1}{2} - \epsilon, \tfrac{1}{2} + \epsilon[\qquad \text{for some} \quad \epsilon \in]0, \tfrac{1}{2}[$$
$$f(\tfrac{1}{2} - x) = f(\tfrac{1}{2} + x) \qquad \text{for} \quad x \in [0, 1]$$

(b)
$$F(\{0\} \times [0, \tfrac{1}{2} - \epsilon]) \subset \{0\} \times [0, 1]$$
$$F(\{0\} \times [\tfrac{1}{2} + \epsilon, 1]) \subset \{1\} \times [0, 1]$$

(c) $|\partial_x g_y(x)| \equiv \lambda < 1/2$ and $|f'| \geqslant \mu > 1$ in $[0, 1] \backslash u$

(c) will ensure some hyperbolicity properties, and fixing $|\partial_x g_y(x)|$ to a *constant* value λ in conjunction with hypothesis (b) will ensure that $F(S)$ has the simple shape represented in Fig. 2a, and allow some explicit computations in the proof of the theorem below.

We shall denote by $\tilde{f}$ the flat-top map defined by

$$\tilde{f}(y) = f(y) \qquad \text{if} \quad y \notin U$$
$$\tilde{f}(y) = f(\tfrac{1}{2} - \epsilon) \qquad \text{if} \quad y \in U$$

Then the following theorem is reminiscent of a result obtained in Ref. 21 for some Hénon mappings. Note however that

i. the formulation is stronger here than in Ref. 21 since we obtain an explicit hyperbolic set;

ii. the case considered here is orientation preserving;

iii. the proof in the present case is quite straightforward.

Theorem. If the topological entropy $h(\tilde{f}) \geqslant \log\sqrt{2}$, then there exists a rectangle R in S such that F^2 acts on R like the genuine horseshoe map. Consequently (i) F^2 acts on some Cantor set in R like the full shift with two symbols; (ii) this Cantor set is in the nonwandering set for F and has hyperbolic structure; (iii) the topological entropy $h(F) \geqslant \mathrm{Log}\sqrt{2}$.

Proof. From $h(\tilde{f}) \geqslant \log\sqrt{2}$, f unimodal, $\tilde{f}$ flat top and $|f'| > 1$ outside of U, one knows that there exists an interval $J = [\tilde{y}, y^*]$ in $[0, 1]$ with

$$\tilde{f}(y^*) = y^*, \qquad y^* \neq 0$$
$$\tilde{f}(\tilde{y}) = y^*, \qquad \tilde{y} < y^*$$

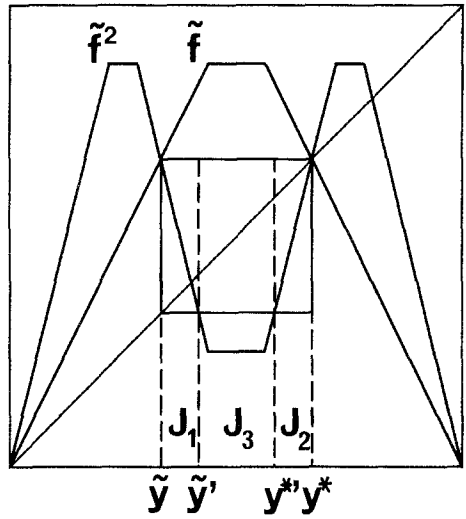

Fig. 3. The points $\tilde{y}$, $\tilde{y}'$, $y^{*\prime}$, y^* as defined in the main text. The mapping is chosen to be piecewise linear for better visualization.

and with the following property P (see Fig. 3):

$$P: \quad \begin{cases} J \text{ contains two disjoint intervals } J_1 = [\tilde{y}, \tilde{y}'], \text{ and} \\ J_2 = [y^{*\prime}, y^*] \text{ such that } \tilde{f}^2(J_i)_{i=1,2} = J \end{cases}$$

Remark. By (a),

$$\tilde{y} = 1 - y^*$$

Let us now consider the rectangle R defined by

$$R = [1 - \lambda, 1] \times J$$

Using (a) (b) (c) and property P, we see that the two horizontal strips in R defined by

$$R_i = [1 - \lambda, 1] \times J_i, \qquad i \in \{1, 2\}$$

are transformed by F^2 into two vertical strips:

$$F^2(R_1) = [1 - \lambda^2, 1 - \lambda^2 + \lambda^3] \times J$$

$$F^2(R_2) = [1 - \lambda + \lambda^2 - \lambda^3, 1 - \lambda + \lambda^2] \times J$$

where we have used the fact that both horizontal strips and their images

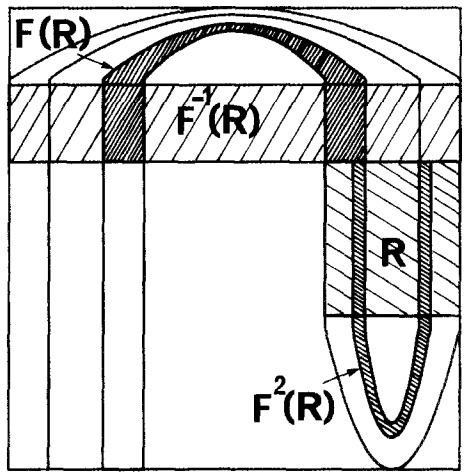

Fig. 4. The two horseshoes for F^2. $F^2(S)$ has also been represented.

under F are in C and that (b) together with $|\partial_n g_y(x)| \equiv \lambda$ yields

$$g_y(x) = \lambda x, \qquad y \leqslant 1/2 - \epsilon$$
$$g_y(x) = 1 - \lambda x, \qquad y \geqslant 1/2 + \epsilon$$

Using now condition (c), and the fact that horizontal lines in R_i are transformed into horizontal lines by F^2, one gets by standard arguments the conclusions listed in the theorem. ■

Remark 1. Under the same circumstances, there exists another horseshoe for $F^2|_{F^{-1}(R)}$ and the nonwandering sets of the two horseshoes are exchanged by F. Both are represented in Fig. 4.

Remark 2. If condition (c) on g is weakened so that

$$|\partial_x g_y(x)| \leqslant \lambda < 1/2$$

the theorem still holds but R is no longer a genuine rectangle; instead, it is given by

$$F[C_R] \cap [0,1] \times J$$

Then, condition (b) is no longer needed and can be dropped.

3.2. Cycles with One Point in the Bad Set

Our main goal, in this subsection, is to illustrate on a specific example how the bifurcation diagram for one-dimensional maps is modified for

invertible mappings. Let us first describe a method for constructing models which display the main features illustrated by Fig. 2a.

Step 1: F Outside the Bad Set. One writes S as a disjoint union:

$$S = C_R \cup [0,1] \times U \cup C_L$$

with $U =]u_m, u_M[$ and choose functions $\tilde{f}$ and a one-parameter family g_y such that in C_R and C_L, F reads

$$F(x, y) = (g_y(x), \tilde{f}(y))$$

Remark. $\tilde{f}$ was defined in Section 3.1 by restricting to $[0,1]\backslash U$ the f of Section 1. Then one gets four points:

$$A = (g_{u_m}(0), \tilde{f}(u_m))$$
$$B = (g_{u_m}(1), \tilde{f}(u_m))$$
$$C = (g_{u_M}(0), \tilde{f}(u_m))$$
$$D = (g_{u_M}(1), \tilde{f}(u_m))$$

It is then simpler to impose that $\tilde{f}(u_m) = \tilde{f}(u_M)$.

Step 2: The Shape of $F([0,1] \times U)$. $F([0,1] \times U)$ will be bounded by the segments $\overline{AC}$, $\overline{DB}$ and two curves $\overset{\frown}{AB}$ and $\overset{\frown}{CD}$. $\overset{\frown}{AB}$ is defined by a map

$$\Gamma_0 : \{0\} \times U \to S$$

$\overset{\frown}{CD}$ is defined by a map

$$\Gamma_1 : \{1\} \times U \to S$$

and in order for $F(S)$ to be U-shaped, $\overset{\frown}{CD}$ must lie above the horizontal line containing A, B, C, D. Then the injectivity of F imposes that $\overset{\frown}{AB}$ be above $\overset{\frown}{CD}$.

Step 3: Getting Formulas for F in $[0,1] \times \overline{U}$. One chooses two monotone decreasing functions:

$$s: [u_m, u_M] \to [0,1] \quad \text{with} \quad s(u_m) = 1, \quad s(u_M) = 0$$
$$t: [0,1] \to [0,1] \quad \text{with} \quad t(0) = 1, \quad t(1) = 0$$

and one writes, for (x, y) in $[0,1] \times \overline{U}$,

$$\begin{pmatrix} x \\ y \end{pmatrix} \mapsto \begin{pmatrix} s(y) \cdot g_{u_m}(x) + [1 - s(y)] \cdot g_{u_M}(x) \\ t(x) \cdot \Gamma_0(\{0\}, y) + [1 - t(x)] \cdot \Gamma_1(\{1\}, y) \end{pmatrix}$$

Step 4: Checking. It remains to check that all parameters used to define g, $\tilde{f}$, Γ_0, Γ_1, s, t, fit together so that F is injective, preserves S, is continuous, and, if necessary, as smooth as one wants. We shall consider the simple case when

i. conditions (a), (b), (c) of the preceding subsection hold;
ii. $\tilde{f}$, s, t are affine functions;
iii. Γ_0 and Γ_1 define parabolas.

This yields

$$F:\begin{pmatrix} x \\ y \end{pmatrix}\to\begin{cases} \begin{pmatrix} \lambda x \\ \mu y \end{pmatrix}, & y \leqslant 1/2-\epsilon \\ \begin{pmatrix} \dfrac{\lambda x(1-2y)+y+\epsilon-1/2}{2\epsilon} \\ A-\delta n-\left[(1-2y)/2\epsilon\right]^2\left[A-\mu(1/2-\epsilon)-\delta x\right] \end{pmatrix} & \text{if } |y-1/2|\leqslant\epsilon \\ \begin{pmatrix} 1-\lambda x \\ \mu(1-y) \end{pmatrix} & \text{if } y\geqslant 1/2+\epsilon \end{cases} \tag{2}$$

where

(a) $0<\lambda<1/2$

(b) $\delta>0, \quad \epsilon>0$

(c) $\mu<\dfrac{2}{1-2\epsilon}$

(d) $\mu>\dfrac{1+2\epsilon}{1-2\epsilon}$

(e) $\epsilon<\dfrac{1}{2}+\dfrac{1}{\mu^2(1+\mu)}-\dfrac{1}{\mu}$

(f) $A\leqslant 1$

(g) $A-S>\mu(1/2-\epsilon)$

(a) and (b) are necessary for F to be injective; (c) and (f) are necessary for S to be invariant under F; (d) gives a nontrivial fixed point out of $[0,1]\times U$; (e), using (d), is equivalent to $h(\tilde{f})>\mathrm{Log}\sqrt{2}$; and (g) is necessary for $F(S)$ to be horseshoe-shaped (f_0 unimodal).

Remark. The local behavior of the f_μ's near $1/2-\epsilon$ and $1/2+\epsilon$ will not play any role for the problems we shall examine in this subsection so that everything will remain valid if instead of the F's we consider smooth mappings obtained by small perturbations in thin strips about $[0,1]\times$

$\{1/2 - \epsilon\}$ and $[0,1] \times \{1/2 + \epsilon\}$ (F itself is a homeomorphism of S onto its image).

We shall examine parts of the bifurcation diagram for one-parameter families F_A, all other parameters in (2) being fixed, and make some comparisons with known results for unimodal maps of the interval. Some kneading theory[3,10] will be useful, both as a tool in some proofs and to make the comparisons possible, so let us recall some facts and fix our notations (see, e.g., Ref. 3 or 10 for justification).

Given a unimodal mapping k of I with critical point c, one associates to each $x \in I$ an itinerary:

$$\mathscr{I}(x) = X_1 X_2 \ldots, X_i \in \{R, L, C\}$$

as follows:

If $k^n(x) \neq c$ for each $n \geqslant 0$ then, for each $n \geqslant 0$,

$$\begin{aligned} X_n &= R, \qquad k^n(x) > c \\ X_n &= L, \qquad k^n(x) < c \end{aligned} \tag{*}$$

If $k^m(x) = c$ and $k^n(x) \neq c$ for each $n < m$,

$$\begin{aligned} X_m &= C \qquad \text{and is the last symbol} \\ (*) &\qquad \text{applies for each } n < m \end{aligned}$$

To each itinerary, one can associate its value $v(\mathscr{I}(x))$ as a decimal number $0, y_1 y_2 \ldots$ in $[0, 2/9]$ as follows:

if y_i is preceded by 0 (respectively, 2) and $X_i = R$,
then $y_i = 2$ (respectively, 0)
if y_i is preceded by 0 (respectively, 2) and $X_i = L$,
then $y_i = 0$ (respectively, 2)
if $X_i = C$ then $y_i = 1$

Then

$$v(\mathscr{I}(x)) < v(\mathscr{I}(x')) \Rightarrow x < x'$$
$$x < x' \Rightarrow v(\mathscr{I}(x)) \leqslant v(\mathscr{I}(x'))$$

The itinerary $k^* = \mathscr{I}(k(c))$ is called the kneading sequence of k: if $h(k) > \operatorname{Log} \sqrt{2}$, then

$$v(k^*) > 0.22020202 \ldots = \frac{218}{990} \tag{3}$$

If k is surjective, then $v(k^*) = 0.222 \ldots = 2/9$, but if $k(c) < 1$, one can always find a N such that, for any itinerary $\mathscr{I}$ beginning by RL^n, $n \geqslant N$:

$$v(\mathscr{I}) > v(k^*)$$

A periodic orbit will be represented by the itinerary of its point with greatest coordinate. (It can happen that infinitely many periodic orbits are represented by a single symbolic sequence, but this does not affect our argument.) The itinerary of a periodic point can be written as the concatenation $\mathscr{I} = \mathscr{I}_n^\infty \equiv \mathscr{I}_n \mathscr{I}_n \mathscr{I}_n \ldots$ indefinitely, of symbolic sequences $\mathscr{I}_n$ formed by the n first symbols of $\mathscr{I}$, where n is the period of the cycle.

For k of class C^1, a cycle is said to be superstable if it contains C; then, Dk^n is zero when evaluated at any of the n points of the cycle. For injective mappings of S, superstability will refer to the cases when DF^n has its spectrum on the imaginary axis and inside the open unit disk.

The cycles of F_A we shall consider correspond, on the interval, to cycles C_n (respectively, $C_{m,p}$) with itinerary RL^nC [respectively, $RL^m(RL)^{2p+1}RC$] when they are superstable and $[RL^{n+1}]^\infty$ {respectively $[RL^m(RL)^{2p+2}]^\infty$} when k is surjective.

The correspondence alluded to above is well defined in our case since we shall only consider cycles with just one point in the bad set $[0,1] \times U$ and thus whose y-dynamics is completely described by a single endomorphism f_ν; and since these cycles are continuous deformation of cycles one gets when $\delta = 0$ or $\epsilon = 0$.

Let $\{k_\alpha\}$ be a C^1-continuous one-parameter family of C^1 unimodal mappings, with $k_{\alpha_{\max}}$ surjective and k_α not surjective for $\alpha < \alpha_{\max}$. As a consequence of Theorem III.1.1 of Ref. 3, there are sequences $\{\alpha_n\}$ (respectively, $\{\alpha_{m,p}\}$, $p > 0$ fixed) converging to $\alpha_{\max}$, such that C_n is superstable for k_{α_n} (respectively, $C_{m,p}$ is superstable for $k_{\alpha_{m,p}}$). Furthermore, $k_{\alpha_{\max}}$ admits all cycles C_n and $C_{m,p}$ (more precisely at least one of each type).

We now remark that $A = 1$ is the largest value of A for which F_A maps S into itself; indeed Proposition 1 below and the remark which follows it will confirm that $A = 1$ is the reasonable counterpart of the $\alpha_{\max}$ we encountered in one-parameter families of one-dimensional maps. We will argue that the above one-dimensional results still hold for the C_n's but not for the $C_{m,p}$'s; this exhibits an explicit modification of the bifurcation diagram known for one-dimensional maps.

Before proceeding, let us recall that since Hénon mappings are area preserving when $|b| = 1$, one gets easily modifications of the one-dimensional bifurcation diagram when $|b|$ is large enough.[1] Using Newhouse's results in Refs. 13 and 14, Van Strien has recently proved[19] that modifications also exist when $|b|$ is small enough. The modifications we shall get work as soon as $\delta \cdot \epsilon \cdot \lambda \neq 0$. Furthermore the approach is much simpler and the modifications are explicit.

Proposition 1 (easy). $A_{\max} = 1$ is the lowest value of A such that there is a tangent homoclinic point in the invariant manifolds of 0 in S.

Remark. This homoclinic tangency thus plays the same role that the "outer" heteroclinic tangency for the Hénon mapping when $b > 0$, as described by Simò in Ref. 18. Simò's analysis would apply to our models adapted to be orientation reversing and the situation is as in Proposition 1 for Hénon mappings when $b < 0$ (orientation preserving case). When $b = 0$ both kinds of tangencies occur simultaneously, when the one-dimensional mapping is surjective.

Lemma 2. There exists a sequence $\{A_n\}_{n\in N}$ converging to 1 such that F_{A_n} admits a superstable cycle RL^nC.

Proof. For $A_n = 1 + \delta\lambda^n(1 - \lambda/2) - 1/2\mu^{n+1}$, one readily verifies that the point $(1 - \lambda/2, 1/2\mu^n)$ belongs to a cycle RL^nC and that this cycle is superstable.

Lemma 3. For n large enough, there exists at least one cycle $[RL^{n+1}]^\infty$ when $A = 1$. More precisely, for such n, one can find a rectangle R_n below the line $y = 1/2$, whose n first images are rectangles disjoint from R_n, below (or partly below) $y = 1/2$, whose $(n+1)^{\text{th}}$ image is above $y = 1/2$ and such that $F_1^{n+2}|_{Rn}$ is a horseshoe.

Proof. It suffices to define R_n by

$$R_n = \left[1 - \lambda, 1\right] \times \left[\frac{1 - 2\epsilon}{2\mu^n}, \frac{1 + 2\epsilon}{2\mu^n}\right], \qquad n \text{ large enough}$$

to get a horseshoe for F_1^{n+2}. In the nonwandering set of this horseshoe, one can find two fixed points for F_1^{n+2}, one to the left of the line $x = 1 - \lambda/2$,

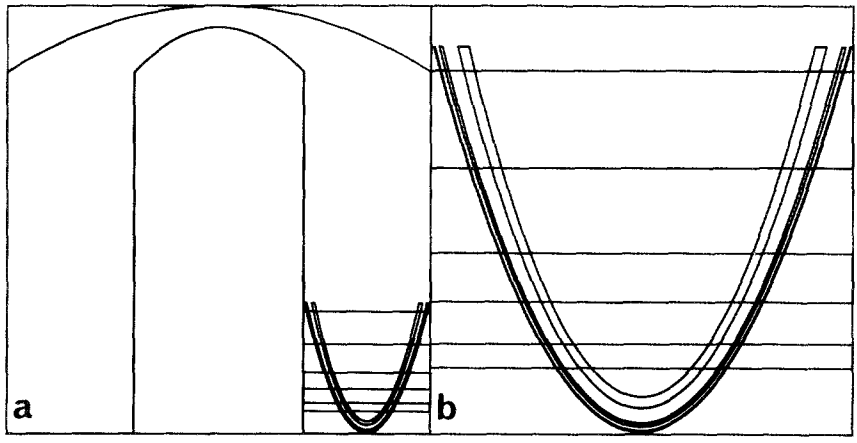

Fig. 5. Four horseshoes for F_1^{n+2}, for $\epsilon = 1/13$, $\mu = 2$, $\lambda = 0.3$, $\delta = 0.05$, and $n = 1, 2, 3, 4$. (a) in S; (b) magnification.

corresponding to the sequence $[RL^nR]^\infty$, one to the right, corresponding to the sequence $[RL^{n+1}]^\infty$. We have represented some of these horseshoes in Fig. 5.

Remark. The case $n = 0$ corresponds to the horseshoe for F_1^2 examined in the previous subsection, so that when

$$\epsilon > \frac{\mu^2 - \mu + 1}{2(\mu^2 + \mu + 1)}$$

the horseshoe for $F_1^3|_{R_1}$ exists and one can take $n \geqslant 0$ in Lemma 3. If ϵ is too small, all horseshoes still exist but the formula for R_n must be modified for small n's.

Lemma 4. For m large enough, all the cycles $[RL^m(RL)^{2p+2}]^\infty$ have exactly one point in $[0, 1] \times U$ for any F_A such that they exist. The same results holds for the cycles $RL^m(RL)^{2p+1}RC$.

Proof. For all points of the cycle, except the one with largest y-coordinate, one verifies that the value of the itinerary is below 218/990 [see (3)] and thus, since $h(\tilde{f}) > \text{Log}\sqrt{2}$, are not in $[0, 1] \times F_A(U)$. Now, $\tilde{f}$ being fixed with $v(k^*) < 0.222 \ldots = 2/9$, it suffices that m be large enough in order for the upper point of the cycle to satisfy $v(\mathscr{S}) > v(k^*)$ and thus to be in $[0, 1] \times F_A(U)$ so that its preimage is in $[0, 1] \times U$.

Now let us remark that the bifurcation diagram of F_A is the same as for one-dimensional mappings when $\delta = 0$ or $\epsilon = 0$. The nature of some changes which occur when $\delta > 0$ and $\epsilon > 0$ is described in the following theorem.

Theorem. For any family $\{F_A\}$ with $\delta > 0$, $\epsilon > 0$, $\lambda > 0$, A varying from some value $A_0 < 1$ to $A_{\max} = 1$, there is a sequence $\{A_n\}_{(n \text{ large enough})}$ converging to 1 such that F_{A_n} admits a superstable cycle RL^nC, and for each such n, there exists at least one cycle $[RL^{n+1}]^\infty$ when $A = 1$. On the contrary, if m is large enough, there is no $A < 1$ such that a cycle $RL^m(RL)^{2p+1}RC$ is superstable for F_A and no cycle $[RL^m(RL)^{2p+2}]^\infty$ exists for a F_A with $A \leqslant 1$.

Proof. By Lemmas 2 and 3, it only remains to prove the negative parts of the theorem. Let us then consider the case of the cycles $[RL^m(RL)^{2p+2}]^\infty$ since the same arguments apply to the $RL^m(RL)^{2p+1}RC$'s. Suppose that a cycle $[RL^m(RL)^{2p+2}]^\infty$ exists for some F_A. A simple computation shows that the point with smallest y-coordinate in the cycle is the one with itinerary $[L^m(RL)^{2p+2}R]^\infty$. Indeed, the y-coordinate of this point must be smaller than $1/2\mu^{(m-1)}$ since its $m - 1$ first iterates are

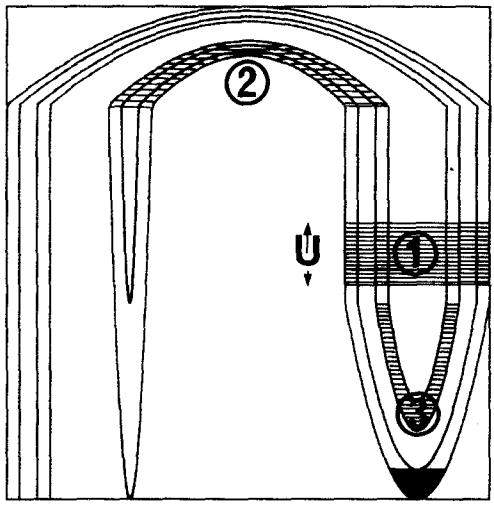

Fig. 6. Representation of $F_1^3(S)$: the points $[XRL^m(RL)^pR]^\infty$, $[RL^m(RL)^pRX]^\infty$ and $[L^m(RL)^pRXR]^\infty$ of $C_{m,p}$ must lie in the shaded areas (1), (2), and (3) respectively, but on the other hand, $[L^m(RL)^pR \times R]^\infty$ should be in the black area for m large enough (X stands for L or R).

below $1/2$ and thus have the y-coordinate multiplied by μ under iteration of F_A.

On the other hand, the preimage $[LRL^m(RL)^{2p+1}R]^\infty$ of the upper point of the cycle must lie in the right vertical strip of $F_A(S)$ (see Fig. 2a): this is due to the fact that its own preimage is $[RLRL^m(RL)^{2p+1}]^\infty$, thus above $[0,1] \times U$ by Lemma 4 and by the fact that the itinerary begins by R. As a consequence, the y-coordinate of the point $[RL^m(RL)^{2p+2}]^\infty$ must be smaller than $A - \delta/2$: its preimage being in the right half of S, this point must have y-coordinate smaller than the upper point of the image $F_A\{1/2\} \times \{0,1\}$ which culminates at $A - \delta/2$. Since, by Lemma 4, the point $[RL^m(RL)^{2p+2}]^\infty$ is in the image $F_A([0,1] \times U)$ of the bad set, conditions (d) and (g) in the formula for F_A imply that it is also above $1/2 + \epsilon$, and the y-coordinate of its image $[L^m(RL)^{2p+2}R]^\infty$ is thus greater than $\mu(1 - A + \delta/2)$.

Since this same point $[L^m(RL)^{2p+2}R]^\infty$ was shown to have y-coordinate smaller than $1/2\mu^m$ at the beginning of the argument, it only remains to remark that, for m large enough, $1/2\mu^m$ is smaller than $\mu(1 - A + \delta/2)$ to get a contradiction. ■

Remark. For maps adapted from the F_A's to the sense-reversing case, the right vertical strip of $F_A(S)$ is mapped above the left vertical strip.

As a consequence, the same kind of arguments as in the proof of the present theorem show that the cycles of type $[RL^m(RL)^{2p+2}]^\infty$ appear before the cycles $[RL^m]^\infty$, when A is increased to the maximal value corresponding to the heteroclinic tangency alluded to in the remark following Proposition 1.

4. EXPLICIT EXAMPLES OF WILD HYPERBOLIC SETS AND INFINITELY MANY SINKS

Let us first recall a definition due to Newhouse.[14]

Definition. Let Λ be a hyperbolic basic set for a C^r diffeomorphism $F: M \to M$ with $r \geqslant 2$ fixed and let U be a compact neighborhood of Λ with $\bigcap_n f^n(U) = \Lambda$. Let us denote by $\Lambda(G)$ the hyperbolic set $\bigcap_n G^n(U)$ for any GC^r-near F. A nondegenerate (parabolic) tangency Z of $W^u(X, F)$ and $W^s(y, F)$ for $x, y \in \Lambda$ will be called a nondegenerate homoclinic tangency for Λ. Then, Λ is a *wild hyperbolic set* if each $G\,C^r$-near F has the property that $\Lambda(G)$ has a nondegenerate homoclinic tangency.

That such sets will occur frequently in the process of formation of a horseshoe is proved by the following theorem.

Theorem (Newhouse[14]). Let $\{F_t\}_{t\in[0,1]}$ be a C^1 curve of C^r diffeomorphisms of M, $r \geqslant 3$ and for each $t \in [0, 1]$, let P_t be a p-periodic point for F_t with $\det T_{P_t} F_{t_0}^P \neq 1$ for some $t_0 \in]0, 1[$ such that $W^u(P_{t_0})$ and $W^S(P_{t_0})$ have a parabolic tangency at some point X. Let U be a neighborhood of X and suppose that in U, $W^u(P_t) \cap W^s(P_t) = \emptyset$ for $t < t_0$, and $W^U(P_t)$ has two transverse intersections with $W^s(P_t)$ for $t > t_0$. Then, for each $\epsilon > 0$ there is a t_ϵ with $|t_\epsilon - t_0| < \epsilon$ such that F_{t_ϵ} has a wild hyperbolic set near the orbit of X.

Robinson[16] recently gave an explicit proof that for some t near t_0, F_t will have infinitely many sinks (this result was implicit in Newhouse's writings, but he had not stated it explicitly).

In this section, our aim is to give explicit examples of the occurrence of both phenomena. The construction of an example with infinitely many sinks will involve only elementary computations but the construction of the wild hyperbolic set will be done using a lemma on the intersection of Cantor sets in $\mathbb{R}$, which also plays a central role in the proof of the above theorem.

Definition.[12] Let K be a Cantor set in $\mathbb{R}$ and K_0 the smallest closed interval containing K. We may write $K_0 - K = \bigcup_{i=0}^{\infty} U_i$, where $\overline{U_i} \cap \overline{U_j} \neq 0$ if $i \neq j$ and each U_i is a bounded open interval. Let U_{-2} and U_{-1} be the unbounded components of $\mathbb{R} - K$. The U_i's, $i \geqslant -2$ are called the K-gaps.

For $i \geqslant 1$, set $K_i = K_0 - \bigcup_{0 \leqslant j \leqslant i-1} U_j$: note that $K = \bigcap_{i \geqslant 0} K_i$. $\{K_i\}_{\geqslant 0}$ is called a defining sequence for K. For $i \geqslant 0$, if K_i^* is the component of K_i containing U_i, $K_i^* \setminus U_i$ is the union of two disjoint intervals C_i^l and C_i^r. Now set

$$\tau(\{K_i\}) = \inf_{i \geqslant 0} \left\{ \min\left(\frac{lC_i^l}{lU_i}, \frac{lC_i^r}{lU_i} \right) \right\}$$

where lI is the length of the interval I. Then

$$\tau(K) = \sup\{\tau(\{K\}) \mid \{K_i\} \text{ is a defining sequence for } K\}$$

is called the *thickness of* K.

We can now formulate the lemma alluded to above:

Lemma.[12,14] Let K and K' be Cantor sets in $\mathbb{R}$ with K in no K'-gap closure and K' in no K-gap closure. If $\tau(K) \cdot \tau(K') > 1$, then $K \cap K' \neq \emptyset$.

The way to use the lemma is to find a hyperbolic basic set Λ and a piece of straight line L such that $W^u(\Lambda) \cap L$ and $W^s(\Lambda) \cap L$ are Cantor sets as above. Then general arguments as given in Ref. 14 show that Λ is a wild hyperbolic set.

4.1. An Explicit Example of Wild Hyperbolic Set

We shall use again the remark that F as defined in Section 3.2 yields smooth mappings by appropriate small perturbations in thin strips about $[0, 1] \times \{\frac{1}{2} - \epsilon\}$ and $[0, 1] \times \{\frac{1}{2} + \epsilon\}$. To simplify the notation, we will only consider one-parameter families F_A as defined in the previous section since apart from smoothness, they satisfy all the conditions of Newhouse's theorem and do have wild hyperbolic sets for some values of A. The wild hyperbolic sets one gets this way can, however, be very small and it is difficult to control them and to prove that one exists for a fixed value of the parameters. Here, we shall adjust the parameters in order to get the horseshoe for F_A^2 as an explicit wild hyperbolic set. The subscript A will be omitted hereafter since we shall have to choose correctly all parameters. Our first task is to investigate the transverse structure of $W^s(\Omega)$ and $W^u(\Omega)$, where Ω is the nonwandering set of the horseshoe described in Section 3.1.

Remark. While $\Omega \cup F(\Omega)$ is a basic hyperbolic set for F, Ω is not. Proving that Ω is a wild hyperbolic set for F^2 will, however, be enough to get $\Omega \cup F(\Omega)$ as a wild hyperbolic set for F.

(a) $W^s(\Omega)$. When $h(\tilde{f}) > \text{Log}\sqrt{2}$ the vertical structure of Ω is completely described by $\tilde{f}^2$ (Section 3.1). To ensure the entropy condition, we

take

$$\mu > \sqrt{2}\,, \qquad \epsilon < \frac{2 + \mu(1+\mu)(\mu-2)}{2\mu^2(1+\mu)}$$

in the definition of F.

Using the notations and results of Section 3.1, let us denote by $J_3 = J \setminus (J_1 \cup J_2)$ the set of points in J whose image under $\tilde{f}^2$ is not in J: then, the projection on the y axis of Ω is obtained by deleting from J, J_3 and all its preimages by $\tilde{f}^2$. This defines a middle-α Cantor set which is constructed like the genuine middle-third, except that the ratio deleted at each step is α instead of one third. For such a Cantor set, one easily gets the thickness:

$$\tau(\alpha) = \frac{1-\alpha}{2\alpha}$$

Here α is the length of J_3 divided by the length of J, i.e.,

$$\alpha = \frac{lJ_3}{lJ} = 1 - \frac{2}{\mu^2}\,.$$

Now, the intersection of $W^s(\Omega)$ with any vertical line in S contains a middle-α Cantor set, say K^s which runs from $y = \tilde{y}$ to $y = y^*$ on the vertical line.

(b) $W^u(\Omega)$. Recall that we chose the rectangle $R = [1-\lambda, 1] \times J$ as the support for the horseshoe of F^2. Now $F^2(R)$ determines in R two vertical strips, respectively, between $1 - \lambda + \lambda^2 - \lambda^3$ and $1 - \lambda + \lambda^2$ and between $1 - \lambda^2$ and $1 - \lambda^2 + \lambda^3$. By iterating this process one determines as usual the transverse Cantor set structure of $W^u(\Omega)$; more precisely, we are dealing with the part of $W^u(\Omega)$ in R whose inverse image under F^2 is also in R, and we obtain that this set can be written as

$$K_0^u \times J$$

where K_0^u is a middle-β Cantor set with extremities $1/(1+\lambda)$ and $(1 + \lambda - \lambda^2)/(1+\lambda)$ and with

$$\beta = 1 - 2\lambda^2$$

so that

$$\tau(K_0^u) \geqslant \frac{\lambda^2}{1 - 2\lambda^2}$$

The image of $K_0^u \times J$ under F cuts the vertical line $x = 1/2$, on a new middle-β Cantor set K_1^u with the same β, by the formula for F which gives an affine mapping from the line $y = 1/2$ to the line $x = 1/2$. K_1^u runs on

$x = 1/2$ between

$$y_{\min,1} = A - \delta\left(\frac{1+\lambda-\lambda^2}{1+\lambda}\right)$$

and

$$y_{\max,1} = A - \delta\left(\frac{1}{1+\lambda}\right)$$

For $n > 1$ small enough, the image $F^n(K_1^u)$ is on the vertical line:

$$x_n = \lambda^{n-1}(1-\lambda/2)$$

It is still a middle-β set K_{n+1}^u which runs from

$$y_{\min,n} = \mu^{n-1}(1 - y_{\max,1})$$

to

$$y_{\max,n} = \mu^{n-1}(1 - y_{\min,1})$$

(c) *An Explicit Example of Wild Hyperbolic Set.* It remains only to choose A, δ, ϵ, λ, μ, and n so that K^s and K_n^u satisfy the conditions of Newhouse's lemma. As an example, one can take $\mu = 1.5$, with $\epsilon = 1/100$ which gives

$$h(\tilde{f}) > \mathrm{Log}\sqrt{2}$$

and

$$\tau(K^s) = 4$$

Then, $\lambda = 0.49$ ensures $\tau(K^u) \simeq 0.4619$, so that $\tau(K^s) \cdot \tau(K_n^u) > 1$. Choosing $n = 3$, it remains to fix A and δ using

$$A = 1 + \frac{\delta}{1+\lambda} - \frac{1}{\mu^2(1+\mu)}$$

which ensures that

$$y_{\min,3} = \tilde{y}$$

This gives the remaining condition of Newhouse's lemma. Using conditions (f) and (g) in the definition of F one can take as an example

$$\delta = 0.1$$

and

$$A = 1 + \frac{\delta}{1+\lambda} - \frac{1}{\mu^2(1+\mu)} \simeq 0.8893$$

Despite the fact that the parameters are explicitly chosen, this example seems less "ad hoc" than Newhouse's original one[12] since it appears on

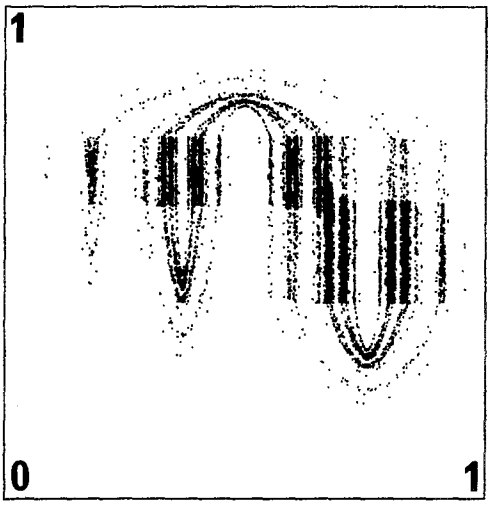

Fig. 7. Numerical simulation of F with parameters as defined in the main text to get a wild hyperbolic set.

the way to a horseshoe. It also allows numerical simulations, as displayed in Fig. 7. Unfortunately, the main information contained in this figure seems to be the confirmation that knowing explicitly a wild hyperbolic set does not help very much to get a global understanding of the mapping.

4.2. Examples of Mappings with Infinitely Many Sinks

The main idea leading to the examples below is to choose maps constructed as explained at the beginning of Section 3.2, in such a way that all periodic cycles corresponding to the kneading sequences RL^nC's, for n large enough, are simultaneously stable. The way these sinks will be organized in the plane will be typical vis-à-vis Newhouse's theory (see Ref. 13, Proposition 3): they will converge to the closure of the set $W^u(0) \cap W^s(0)$. However, because of the simple structure of these periodic orbits, the fixed point 0 will not be dissipative, i.e., the product of the eigenvalues of the linearized mapping at 0 will be equal to 1. It is our opinion that this should not be dramatic for the numerical observability of the phenomenon.

The examples are constructed as follows.

Case One. One uses F_1, i.e., F as defined in Section 3.2 with $A = 1$, then one writes the conditions of coexistence of all RL^nC's. Using the proof of Lemma 2, this reads

$$n \geqslant 1 \Rightarrow 2\delta\mu^{n+1}\lambda^n(1 - \lambda/2) \equiv 1$$

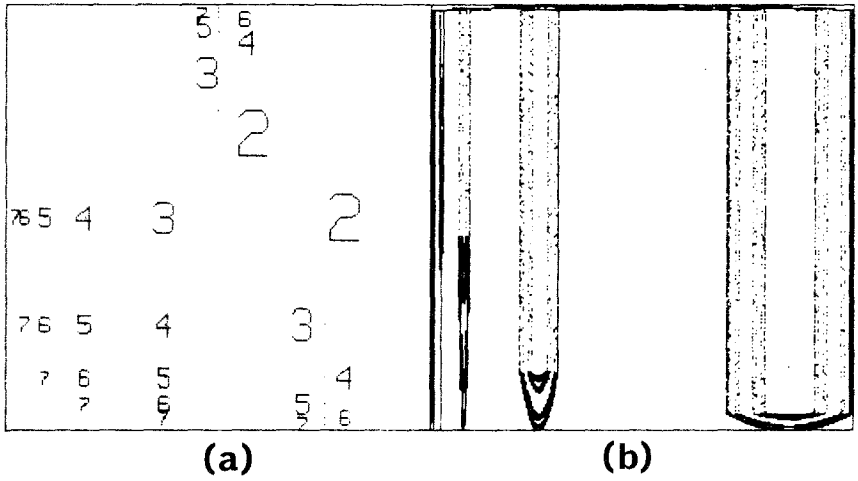

Fig. 8. Numerical simulations of mappings with infinitely many sinks: (a) and (b) correspond to cases 1 and 2 of the main text.

Thus, one must set

$$\mu\lambda = 1$$

and

$$\delta = \frac{1}{\mu(2 - \mu^{-1})}$$

Such an example has been illustrated in Fig. 8a. Here, $\epsilon = 0.2$ and $\mu = 2.01$ so that $\lambda \simeq 0.4975$ and $\delta \simeq 0.3311$. In this case, one can visualize all sinks RL^nC up to $n = 18$ with a computer HP.9845-B.

For greater n's, starting from the best numerical approximation of a point of the cycles (our computer uses 12 digits), numerical errors eventually cause divergences: for many examples of the same kind, one converges to 0 or one of the sinks of low period when starting near a sink of high period.

Case Two. By choosing correctly a $\tilde{f}$ with nonconstant slope in Step 1 of the construction of F in Section 3.2, we can avoid the cycles corresponding to the RL^nC's with n small while keeping infinitely many sinks corresponding to the RL^nC's with n large enough. The effect in a numerical simulation is that, instead of converging to a known stable cycle as in the preceding case, one can converge to some uncontrolled apparently strange attractor as illustrated in Fig. 8b with the simplest case of a piecewise affine $\tilde{f}$.

ACKNOWLEDGMENTS

Thanks to a visit of one of them (Charles Tresser) to the Institute for Mathematics and its Applications in Minneapolis, the authors have benefited from infinitely many hints given by Professor O. Lanford, for the improvement of a wild version of this manuscript.

REFERENCES

1. A. Arneodo, P. Coullet, C. Tresser, A. Libchaber, J. Maurer, and D. D'Humières, *Physica* **6D**:385 (1983).
2. R. Bowen, *On Axiom-A Diffeomorphisms* (Conf. Board of the Math. Sci. Regional Conf. no. 35, 1978).
3. P. Collet and J. P. Eckmann, *Iterated Maps of the Interval as Dynamical Systems* (Birkhauser, Boston-Basel-Stuttgart, 1980).
4. J. Curry, *Commun. Math. Phys.* **68**:129 (1979).
5. J. Curry, *J. Stat. Phys.* **26**:683 (1981).
6. R. Devaney and Z. Nitecki, *Commun. Math. Phys.* **67**:137 (1979).
7. V. Franceschini and L. Tebaldi, *J. Stat. Phys.* **25**:757 (1981).
8. M. Hénon, *Commun. Math. Phys.* **50**:69 (1976).
9. F. Marotto, *Commun. Math. Phys.* **68**:187 (1979).
10. J. Milnor and W. Thurston, On Iterated Maps of the Interval I, II, Preprint, Princeton (1977).
11. M. Misiurewicz and B. Szenc, *Commun. Math. Phys.* **75**:285 (1980).
12. S. Newhouse, in *Global Analysis* Proceed. Pure Math. A.M.S., Vol. 14, p. 191 (1971).
13. S. Newhouse, *Topology* **12**:9 (1974).
14. S. Newhouse, *Pub. Math. I.H.E.S.* **50**:101 (1979).
15. S. Newhouse and J. Palis, in *Dynamical Systems*, M. M. Peixoto ed. (Academic Press, New York, 1973).
16. C. Robinson, Bifurcation to Infinitely many Sinks, Preprint, Northwestern University 1982.
17. D. Ruelle and F. Takens, *Commun. Math. Phys.* **20**:167 (1971); **23**:343 (1971).
18. C. Simò, *J. Stat. Phys.* **21**:465 (1979).
19. J. Van Strien, in *Dynamical Systems and Turbulence*, Warwick 1980, D. A. Rand and L. S. Young, eds. (Springer Lecture Notes in Math. no. 898, Springer, Berlin, 1981).
20. S. Smale in *Differential and Combinatorial Topology* S. Cairns, ed. (Princeton University Press, Princeton, New Jersey 1965).
21. C. Tresser, A. Arneodo, and P. Coullet, Letter to the Editor, *J. Phys.* **A13**:L-123 (1980).

Added in proof: the reader should also consult

22. P. Holmes and D. Whitley, Bifurcations of one and two dimensional maps. Preprint, Cornell Univ. (1983) (received while proofreading).